Engineering 34 (2024) 233–245

Contents lists available at ScienceDirect

Engineering

journal homepage: www.elsevier.com/locate/eng

Research
Large-Scale Energy Storage—Article

Characteristics Analysis of Integrated CAES and CFPP Trigeneration System Considering Working Conditions and Application Scenarios

Jiajia Li, Peigang Yan, Guowen Zhou, Xingshuo Li, Qiang Li, Jinfu Liu *, Daren Yu

School of Energy Science and Engineering, Harbin Institute of Technology, Harbin 150001, China

ARTICLE INFO

Article history:
Received 14 September 2022
Revised 9 June 2023
Accepted 13 June 2023
Available online 13 October 2023

Keywords:
Compressed air energy storage
CFPP–CAES combined cycle
Thermodynamic performance
Technical economics

ABSTRACT

To meet the goal of worldwide decarbonization, the transformation process toward clean and green energy structures has accelerated. In this context, coal-fired power plant (CFPP) and large-scale energy storage represented by compressed air energy storage (CAES) technology, are tasked with increasing renewable resource accommodation and maintaining the power system security. To achieve this, this paper proposes the concept of a CFPP–CAES combined cycle and a trigenerative system based on that. Considering the working conditions of the CFPP, thermal characteristics of three typical operation modes were studied and some general regularities were identified. The results of various potential integration schemes discussion indicated that extracting water from low-temperature points in the feedwater system to cool pressurized air and simultaneously increase the backwater temperature is beneficial for improving performance. In addition, preheating the pressurized air before the air expanders via low-grade water in the feedwater system as much as possible and reducing extracted steam contribute to increasing the efficiency. With the optimal integration scheme, 2.85 tonnes of coal can be saved per cycle and the round-trip efficiency can be increased by 2.24%. Through the cogeneration of heat and power, the system efficiency can reach 77.5%. In addition, the contribution degree of the three compression heat utilization methods to the performance improvement ranked from high to low, is preheating the feedwater before the boiler, supplying heat, and flowing into the CFPP feedwater system. In the cooling energy generation mode, the system efficiency can be increased to over 69%. Regardless of the operation mode, the benefit produced by integration is further enhanced when the CFPP operates at higher operating conditions because the coupling points parameters are changed. In addition, the dynamic payback period can be shortened by 11.33 years and the internal rate of return increases by 5.20% under a typical application scenario. Regarding the effect of different application scenarios in terms of economics, investing in the proposed system is more appropriate in regions with multiple energy demands, especially heating demand. These results demonstrate the technical advantages of the proposed system and provide guiding principles for its design, operation, and project investment.

1. Introduction

Globally, energy policies are moving rapidly toward renewable, efficient, and flexible energy systems to address the increasingly accelerated pressure produced by climate changes and fossil fuels shortage problems [1]. In this context, renewable energy is being vigorously developed and is predicted to generate the same amount of energy as coal and gas-fired power in the global energy supply framework by 2040 [2]. Because renewable energy is not as high-value and controllable as conventional power due to its natural characteristics, its incorporation into the grid poses substantial challenges to the power system in terms of maintaining system operation security and stability. Therefore, enhancing the regulation capacity and flexibility of the power system while reducing regulation expenses as much as possible is essential.

Coal-fired power plants (CFPPs) are the current main source of dispatchable energy units in most countries such as China; hence, their role in the power grid is evolving from conventional power generation units to major regulating resources. Many policy documents guiding energy development directions of energy indicate

* Corresponding author.
E-mail address: jinfuliu@hit.edu.cn (J. Liu).

https://doi.org/10.1016/j.eng.2023.06.015

that CFPPs should take the lead in the power system to fully use coal, provide reliable capacity as well as ancillary services, and aid in green energy development to help the vision of a transformation to low-carbon and sustainable energy system [3,4]. However, standalone thermal power plants experience problems with low-load stable combustion in boiler, poor economy, and safety during deep peak-shaving operations, as well as requiring frequent and wide-range adjustments [5–7].

Energy storage systems (ESSs) can shift energy through storage and delivery processes and provide fast response. As highly flexible resources, ESSs are playing a crucial role in the energy revolution. Equipping a CFPP with a large-scale ESS is a feasible method for considerably increasing its flexibility and transitioning to the new power system. Among the mainstream ESS technologies, compressed air energy storage (CAES) provides many advantages in terms of large capacity, security, eco-friendliness, long service life, low cost, and the lack of geographical constraints. Hence, CAES is regarded as a promising ESS technology [8,9]. Interest in CAES technology began in the 1970s. Two commercialized CAES plants have been installed: the Huntorf plant in Germany and the McIntosh plant in the United States [10]. Recently, many milestones in the development of 10–100 MW level compressed air storage technology have been achieved [11], indicating that CAES technology has a promising future. However, due to the working mechanism of CAES, its efficiency is not very high and the cost of adjustment is higher than that of conventional generation resources, which limits its marketing and engineering application.

To enhance the CAES efficiency, many novel systems and modifications have been proposed and studied. Novel systems such as adiabatic CAES, thermal energy storage (TES), isothermal CAES, supercritical CAES, and hybridization have been proposed [11]. For system modifications, the inter-stage cooling of multiple-compressions and the heating of multiple-expansion structures have been proposed to benefit from the isothermal approach [12]. Considering the limitations of Huntorf plant, such as the time of operation and process constraints, Jafarizadeh et al. [13] proposed and compared four modification methods to enhance the plant performance including regeneration, compressors cooling, application of water injection, and utilization of steam injection. The results showed that they would improve the plant round-trip efficiency (RTE) by approximately 37.80%, 3.22%, 2.50%, and 2.78%, respectively, compared with that of the original plant. It is noted that the peculiar working mechanism of CAES system provides its natural ability to generate, convert, and supply multiple energy sources, which is different from other typical energy storage types. Hence, in addition to the improvement in each component and the entire system, the open features in the thermal process and flexible layout structure enable it the potential to integrate with other cycles. The existing research results of the integration of CAES with other systems or cycles, such as ammonia–water absorption refrigeration system and organic Rankine cycle [14,15], gas turbine [16], and solar and seawater desalination system [17], demonstrated that reasonable incorporation may enable improved energy use and even increase system economic performance.

Inspired by this, the incorporation of thermal power plants and CAES systems may provide a solution to compensate for their respective shortcomings, producing complementary advantages through cycle integration and energy efficient use. That is, the CAES system enlarges the adjustment range, reduces shutdowns and rapid ramping frequency, and relieves the adjustment pressure on the thermal power plants, strengthening its regulation ability. In addition, the CAES system more effectively use energy and improve performance. Its economic viability may also be improved through resources sharing with existing thermal power plants. Hence, integration makes it more competitive in marketing and applications.

To the best of our knowledge, existing work on the integration of coal-fired thermal power plants and CAES systems is rare. Pan et al. [18] integrated a 350 MW coal power plant and a CAES system to improve the performance of a conventional CAES system. The compression heat of the CAES system was transferred to the feedwater of a thermal power plant, and parts of the feedwater of the thermal power plant were employed to preheat the pressurized air before it entered the expanders during the discharge process. The RTE and exergy efficiency of the new CAES system were 64.08% and 70.01%, respectively. Zhang et al. [19] compared different possible coupling schemes of a 660 MW supercritical CFPP and a 50 MW CAES system. Similarly, others [20–22] also focused on the integrated system performance and all of them chose the RTE as the evaluation index to determine the optimal integration. The main differences between these studies were the technical parameters of the system and the integration principle.

From the aforementioned analysis, there exist some limitations in the current research. The study on the incorporation of CFPPs and CAES systems is still in the preliminary stage and the related studies are scarce. The internal coupling mechanism of these two systems as well as system characteristics have not yet been thoroughly studied. In addition, the existing studies have been conducted based on a fixed CFPP working condition. However, the cooperation between the CFPP and CAES systems changes to meet the actual demand. Hence, the effect of the conditions on the thermodynamic process should be examined. Overall, more theoretical research is required to gain a deeper understanding of this new integrated system. In addition, the existing work concentrated only on power generation scenarios. Considering the natural trigeneration potential of CAES system, there is a gap in the study of system integration considering comprehensive energy use in scenarios with multiple energy production. Finally, only the thermal performance has been evaluated. As a new system, the economic perspective is equally important. To fill these gaps, this paper first analyzed the mechanism of the integration of the two systems from a thermodynamic perspective. Based on this, this paper put forward an advanced trigenerative system. Using the developed energy flow models and considering the working conditions of the CFPP, the thermal characteristics and performance of the system were explored and analyzed. Furthermore, a detailed techno-economics comparison analysis was also conducted to evaluate the feasibility of the marketing and application of the proposed system. This study provides deep insights into the advanced integration, quantitatively assesses the system advantages and also gives a guiding principle for design, operation, and project investment. The major originality and contributions of this study are threefold:

(1) The CFPP and CAES integration mechanisms were analyzed to reveal their thermodynamic essence and technical advantages. Subsequently, an advanced trigenerative system based on that was put forward.

(2) System performance and thermal characteristics were separately studied and discussed for three typical operation modes under different working conditions to obtain deep insights into the new system. Moreover, general regularities were refined and summarized to guide system design and operation.

(3) Using the specially established economic calculation model for a CAES system incorporated with a CFPP, a comparative techno-economics evaluation was conducted. In addition, the effect of various application scenarios on economic values was discussed to explore the investment potential for the system in different regions.

The remainder of this paper is organized as follows: The integration thermodynamic mechanism of the CAES system and CFPP is analyzed in Section 2. Accordingly, a novel trigenerative

integration system is presented in Section 3. The mathematical model and evaluation indexes of the proposed system are given in Section 4. In Section 5, we present a thermal characteristics analysis of three typical operating modes under different working conditions. Next, a comparative techno-economics analysis is carried out and the effects of application scenarios are studied in Section 6. At last, the conclusions are drawn in Section 7.

2. Thermodynamic mechanism of CFPP–CAES integration

2.1. Mechanism analysis

The allocation of an electric storage system is an effective way for enhancing the regulation ability of thermal power units. Many researches and engineering applications have demonstrated this point [23,24]. However, the existing work mostly concentrate on frequency modulation improvements; only small-capacity ESS such as batteries have been adopted. To increase the flexibility of thermal power plants, long-term, large-scale, and low-cost ESSs with flexible selection addresses are required. After a comprehensive comparison of the existing common technologies, we developed the idea of installing a CAES for CFPPs.

Compared with conventional CAES technology, the adiabatic CAES (A-CAES) system recovers and stores the heat generated during the compression stage in the TES system and uses it during the discharge process to preheat the expander inlet air as shown in Fig. S1 in Appendix A. This means that A-CAES technology is less dependent on fossil fuels and more environmentally-friendly, so is in alignment with the development direction toward energy savings and emission reductions. However, the performance of a standalone A-CAES system heavily relies on heat storage technology, and the latter increases construction costs [25] and heat loss in the heat capture and use process. Furthermore, compression heat restricts the power generation ability of air expanders. As a result, the goal efficiency of standalone A-CAES system is only 70%, which is much lower than these high-efficiency energy storage technologies such as batteries and pumped hydro energy storage [26].

From a thermodynamic point of view, CAES system is similar to an open-circuit gas turbine plant but with a decoupling compression and expansion process. Hence, the measures used in gas turbines to increase the efficiency from the thermodynamic mechanisms, such as intercooling, regeneration, reheating, and their combination, can provide a reference for CAES system. Many CAES modifications have thus been inspired. Considering the inherent restrictions in the charge and discharge processes of standalone A-CAES systems, in addition to their own optimization, a reasonable integration with the CFPP cycle breaks the inherent constraints and provides a feasible solution to more comprehensively use energy. For example, Fig. S2 in Appendix A presents the diagram of temperature variation in working process of a standalone 50 MW CAES system based on Ref. [27] and a typical 350 MW thermal power unit. Both of these two systems have complex structures with multiple stages and wide ranges of temperature grades. The diagram shows that the temperature range of the CAES system is entirely covered by that of the CFPP. This implies that the generated compression heat can flow into the steam and water circulation of the CFPP based on the principles of temperature matching and cascade use. Similarly, the heat absorbed by air during the discharge process can be extracted from a suitable point of the CFPP to satisfy the preheating demand. After integration, this not only promotes the more reasonable use of the recovered compressed heat but also decouples the natural restrictions of thermal energy in terms of quantity and quality between the charge and discharge subsystems.

From the aforementioned analysis, the integration of CAES and CFPP provides opportunities for thermal cycles and performance improvement. In general, the complex structure of a CFPP provides multiple combination points for a wide range temperature grade. This provides sufficient flexibility for the integration of CAES for various purposes. This means that the integration not only has the potential to increase thermal economy through the application of technologies used to improve gas turbines performance but can also derive modifications and new forms to produce additional benefits.

Based on this, we define their integration as a CFPP and CAES system combined cycle (CFPP–CAES combined cycle). Further explanations of the proposed CFPP–CAES combined cycle are provided. Unlike conventional combined cycles, such as the gas-steam combined cycle [28], the bottom cycle is driven by the top cycle and they are not independent. In the CFPP–CAES combined cycle, energy interactions occur between the two cycles to increase the effectiveness of energy use. Both the ESS and the thermal power unit can operate separately. They can tightly couple with each other or partially decouple, with high freedom and flexibility, to better satisfy the needs of actual operation scenarios. Hence, the CAES cycle is regarded to be inserted into the CFPP cycle as a patch, and their integration is an effective method for the sustainable development of both CAES technology and CFPP to play a substantial role in the energy structure transformation process. The wide temperature variation range, as well as the plenty possible combination points in a CFPP provides great flexibility and freedom in system design and optimization to realize different purposes and benefits. Based on the above analysis, for the integration of CAES and CFPP, except for the basic design principle of temperature matching and cascade utilization, the system design and operation should be modified considering the specific application scenarios demand and features.

2.2. Technical advantages

The integration of a CAES system into a CFPP with multiple energy interactions is expected to have advantages in three aspects:

(1) Enhancing regulation ability. The energy absorption and release abilities of the CAES system enlarges the operation domain of CFPP. Both the minimum and maximum power generation are enhanced. In addition, the fast response of the CAES system complements the CFPP in multiple-time scale power regulation. Less frequent shutdowns and fast ramping can be realized.

(2) Increasing the thermal economy. Compression heat can be more appropriately used after integration with a CFPP. In addition, the technical parameters restrictions between the charge and discharge subsystems are overcome, enabling a more flexible CAES system design and more efficient operation to realize better performance.

(3) Better economy performance. For the CFPP, the regulation pressure is reduced with the help of CAES system; hence, the lifetime of the plant components can be extended. For the CAES system, the integration cuts down the investment cost in heat storage. In addition, the existing supporting facilities and personnel in the thermal power plant can be shared. With reasonable resource allocation, the land acquisition and labor costs of the CAES system can be reduced. In addition, facing specified scene characteristics and needs, the system can provide more energy products through adjusting system operation mode, and the economic benefits can be further improved.

3. Description of a trigenerative CFPP–CAES system

In this paper, a trigenerative system based on the CFPP–CAES combined cycle was proposed and studied. A typical 350 MW subcritical thermal power unit and a 20 MW CAES system were selected as the study objects. The main parameters of this CAES system refers to Ref. [27]. The main parameters in the design point are displayed in Tables 1 and 2.

The schematic of the integrated trigenerative system is illustrated in Fig. 1. It has three main operational modes to face different scenario requirements.

(1) Mode 1: power generation. The power generation mode is applicable to scenarios without heat or cooling demands, such as transitional seasons or regions with a comfortable climate. Under these circumstances, excess electricity drives the compressors work and converts electric energy into pressure and thermal energy. Instead of setting up an additional heat storage tank, the high-temperature pressurized air exchanges heat with condensed water or feedwater to use the compression heat in the thermal power unit. After cooling, the air flows into the air storage tank for later use. To achieve the reasonable cascade use of compression heat, three-stage intercoolers are adopted, and their cold sources are water from different points in the CFPP feedwater system. Fig. 1 shows the proposed integrated system structure under one possible scheme. A_{in}, B_{in}, and C_{in} refer to the extraction locations of the cold source from the CFPP feedwater system for three-stage intercoolers; A_{out}, B_{out}, and C_{out} are their combination locations after heat exchange with the CAES system, respectively. During peak times, the CAES system runs in discharge mode and jointly supplies electricity with the CFPP. Under these conditions, pressurized air is released and preheated by the thermal power unit to strengthen its working ability. Similarly, two heaters are adopted before each expander to perform cascade heating. The hot resources of the low- and high-temperature heat exchangers are feedwater and steam, respectively. D_{in} and E_{in} are the hot source location of the two preheaters from the CFPP; D_{out} and E_{out} refer to their injection points after heating air, respectively. These combination points have many options that will have different effects on system performance. Hence, detailed scheme descriptions are displayed in later sections and are specifically discussed, compared, and analyzed.

(2) Mode 2: cogeneration of heat and power. In winter or cold regions, users have both daily hot water and heating demand, and the total heat load is high. In this scenario, the system can switch to the cogeneration of heat and power mode. In the charging process, instead of injecting all the recovered compression heat into the feedwater system, low-grade compression heat is used to supply heat for users, whereas the medium- and high-temperature portions are used as in the Mode 1. As the heat load increase, the amount of heat exchange among the three-stage intercoolers can be changed to meet actual demand and pursue for better benefit. In the discharge process, the integration form of the CAES system with CFPP and the operation mechanism are the same as Mode 1. The CAES system is activated to release the stored energy and enhance the total on-grid power capacity of the CFPP.

(3) Mode 3: cogeneration of cooling and power. This mode is applicable in scenarios with both electricity and cold energy demands, such as during summer or in hot regions. The generated compression heat is completely injected into the steam and water circulation during the charge process, as illustrated in Mode 1. In the discharge stage, the heat absorption from the CFPP is regulated to reduce the air outlet temperature and supply cooling energy.

Table 1
Design technical parameters of CAES system.

Parameter	Value
Ambient pressure (MPa)	0.1013
Ambient temperature (°C)	20
Total power consumption (MW)	15
Total power generation (MW)	20
Isentropic efficiency of compressor (%)	88
Isentropic efficiency of expander (%)	88
Compression ratio	8.31
Expansion ratio	7.01
Charge time (h)	4.76
Energy storage pressure (MPa)	7
Energy release pressure (MPa)	5

Table 2
Design technical parameters of CFPP.

Parameter	Value
Main steam mass flow rate ($t \cdot h^{-1}$)	1040.79
Main steam pressure (MPa)	16.7
Main steam temperature (°C)	537
Power load (MW)	350
Reheat steam pressure (MPa)	3.259
Reheat steam temperature (°C)	537
Exhaust steam backpressure (MPa)	0.0049

4. Model development

4.1. Thermodynamic analysis model

4.1.1. CAES system model

For a conventional A-CAES system, the main components include multiple-stage air compressors and expanders, heat exchangers, air storage tanks, and thermal storage devices. After integration with a CFPP, the heat storage tank is removed because the recovered compression heat is directly used. The following assumptions are made in this study to simplify the model: ① Air is treated as an ideal gas that conforms to the ideal gas state equation. ② Both the compression and expansion processes in the compressors and expanders are adiabatic. ③ The heat dissipation and pressure loss of the working medium in pipelines are ignored. ④ The throttling process is isenthalpic. The models used in this paper were mainly developed from previous study [29,30], which were experimentally validated. The system off-design characteristics are also considered in modeling [31,32]. Detailed model of each component in the system can be found in Section S2 in Appendix A.

Under the multiple energy cogeneration modes, the heat and cooling energy output ($Q_{heat,out}$ and $Q_{cool,out}$) can be calculated with Eqs. (1) and (2).

$$Q_{heat,out} = \int_0^{t_{ch}} m_c(h_{c,in} - h_{c,out})dt \quad (1)$$

$$Q_{cool,out} = \int_0^{t_{dis}} m_e(h_{e,out} - h_{e,in})dt \quad (2)$$

where t represents the duration time; the subscript "ch" and "dis" represent the charging and discharging phase, respectively; m is the air mass flow rate, $kg \cdot s^{-1}$; h is the air enthalpy, $kJ \cdot kg^{-1}$; the subscript "c" and "e" denote the compression and expansion process; and the subscript "in" and "out" represent the air flow directions to supply heating/cooling energy.

4.1.2. CFPP model

For the CFPP, the mass and energy balance equations were used, followed by empirical relationships for the working substance properties and extraction pressure for the bled steam. On the basis

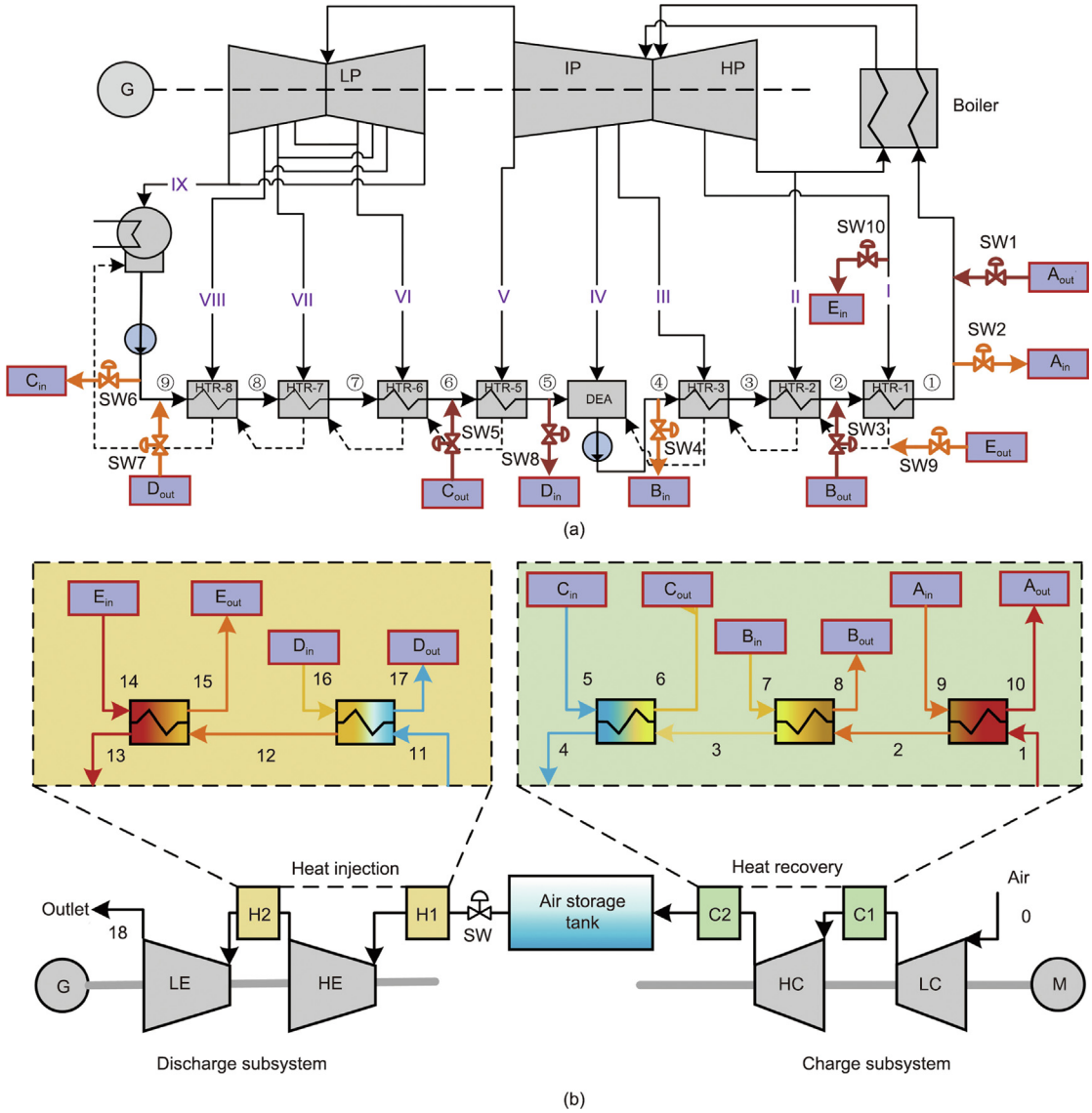

Fig. 1. Schematic of proposed trigenerative system based on CFPP–CAES combined cycle. (a) CFPP and (b) CAES system. G: generator; LP: low-pressure cylinder; IP: intermediate-pressure cylinder; HP: high-pressure cylinder; SW: switch; HTR: feedwater heater; DEA: deaerator; C1: #1 air cooling system; C2: #2 air cooling system; H1: #1 air heating system; H2: #2 air heating system; LE: low-pressure air expander; HE: high-pressure air expander; HC: high-pressure air compressor; LC: low-pressure air compressor; M: motor; A_{in}, B_{in}, and C_{in} refer to the extraction locations of the cold source from the CFPP feedwater system for three-stage intercoolers; A_{out}, B_{out}, and C_{out} are their combination locations after heat exchange with the CAES system, respectively; D_{in} and E_{in} are the hot source location of the two preheaters from the CFPP; D_{out} and E_{out} refer to their injection points after heating air, respectively.

of Ref. [33], the detailed formulations of coal-fired power unit considering integrating with CAES system are presented in Section S2 in Appendix A.

4.1.3. Model validation

The CAES system models were validated by comparing the simulation results to the design data in the reference study [27]. The results of the main parameters were obtained and compared with those of the associated publication as shown in Table S1 in Appendix A. As for the model validation of the CFPP, the validation results of a 350 MW power plant compared with the data from the manufacturer under different working conditions were listed in Table S2 in Appendix A. The maximum error of the calculated results was acceptable. Hence, the models could meet the accuracy requirements of thermodynamic analysis.

4.1.4. Thermodynamic index

System power efficiency (SPE) and RTE were adopted to evaluate the performance of CAES system before and after integration with the CFPP [34,35].

SPE is defined as the ratio of the total electricity output of the CAES system during the discharge process to the input electricity in the charge stage. It describes the electric energy conversion efficiency of the ESS. Because the working state of the thermal power unit changes after integration, the changes of power generation in the two processes were also considered in the index calculation, as shown in Eq. (3).

$$\mathrm{SPE}=\frac{\int_0^{t_{\mathrm{dis}}}(P_{\mathrm{e}}+P_{\mathrm{CFPP,dis}}-P_{\mathrm{CFPP,dis,0}})\mathrm{d}t}{\int_0^{t_{\mathrm{ch}}}(P_{\mathrm{c}}+P_{\mathrm{CFPP,ch,0}}-P_{\mathrm{CFPP,ch}})\mathrm{d}t} \tag{3}$$

where P is the power consumption or generation, kW; the subscript "0" denotes the original CFPP without integration.

RTE is used to evaluate the system from multiple energy complementation and comprehensive use perspectives. It is defined as the ratio of the total energy output to the input. Similarly, the positive and negative effects of system integration on the thermal power unit were considered in the index calculation. On the basis of the SPE, the energy output also includes the production of heat energy Q_{heat} and cooling energy Q_{cool}. Because the energy use may lead to the result of RTE over 1 based on the first law of thermodynamics, all the energy inputs and outputs are converted into electricity to simplify the calculation. Specifically, cooling and heating supplies are converted into electricity savings by producing the same amounts of energies using the conventional heat pumps. cop_{heat} and cop_{cool} are their respective performance coefficients, and they are considered equal to 3.5 and 3.0 respectively as proposed by Ref. [36] as an approximation. In addition, the coal consumption of the CFPP boiler is changed owing to the thermal integration with the CAES system. The equivalent power generation or consumption by coal change was calculated using heat rate, which is defined as the ratio of total boiler heat absorption and total power generation. The calculation formulas are as follows:

$$\mathrm{RTE}=\frac{\int_0^{t_{dis}}\left[\left(P_e+P_{CFPP,dis}-P_{CFPP,dis,0}\right)+\frac{Q_{cool}}{cop_{cool}}+\Delta P_{equi,dis}\right]dt+\int_0^{t_{ch}}\frac{Q_{heat}}{cop_{heat}}dt}{\int_0^{t_{ch}}\left(P_c+P_{CFPP,ch,0}-P_{CFPP,ch}-\Delta P_{equi,ch}\right)dt} \tag{4}$$

$$\Delta P_{equi}=3600\times\left(Q_{boiler,0}-Q_{boiler}\right)/HR_0 \tag{5}$$

where Q_{boiler} denote the heat absorption by boiler, kW; HR is the heat rate of CFPP, $kJ{\cdot}kW^{-1}{\cdot}h^{-1}$; the subscript "equi" denotes the equivalent power caused by the fuel consumption variation before and after integration with CAES system.

4.2. Economic analysis model

4.2.1. Cost model

The cost of the CAES system after integration consists of the initial investment cost C_{fixed} and later operational costs C_{ope} [37]. The initial investment cost can be further divided into equipment purchase C_{eq}, land acquisition C_{land}, and factory construction costs C_{con}. The operation cost can be separately divided into electricity costs C_{ele} for energy storage, equipment maintenance C_{ma}, and labor costs C_{labor}. The cost model of the CAES system is expressed as follows:

$$C_{fixed}=C_{eq}+C_{land}+C_{con} \tag{6}$$

$$C_{ope}=C_{ele}+C_{labor}+C_{ma} \tag{7}$$

(1) Equipment cost. The main components of a standalone CAES system include multiple stages of compressors, expanders, intercoolers, heat exchangers, and thermal and cold storage tanks. The cost functions were listed in Table S3 in Appendix A [38,39]. It should be noted that the investment in thermal storage tanks can be reduced after integrating with the thermal power unit.

(2) Land acquisition and factory construction cost. The land acquisition cost can be estimated by multiplying the land price by the area covered. Sharing the land resources in the thermal power plant is beneficial for reducing these investments. We assumed that after integration, the land acquisition and labor costs were reduced to 80% of those in standalone operation mode.

(3) Operation cost. The maintenance cost is approximately 1%–5% of the fixed investment cost for a CAES system [40]. The labor cost can be determined from the number of workers and salary for each person per year. Similarly, human resources can also be shared after integration, resulting in a decrease in operational costs. In addition, the complex integration will aggravate the operation and maintenance burdens. Hence, a higher maintenance cost coefficient was selected for the integration mode as an approximation.

(4) Electricity cost for energy storage. The electricity cost for energy storage refers to the cost of the energy consumption in the charging phase. A standalone CAES system always buys valley electricity from the power system and sells the electricity generated during the discharge process at peak times to arbitrage. Hence, the energy storage cost was calculated using electricity consumption and the valley electricity price. For the same ESS after integration, it absorbs the electricity produced by the thermal power unit, which leads to a reduction in the on-grid power. Hence, the cost of energy storage is defined as the benefit reduction of selling electricity of the CFPP caused by integration with the CAES system.

4.2.2. Benefit model

In the standalone operation mode, the benefit provided by the CAES system is from the power grid by selling the produced electricity in the discharge phase. After integration, the income from energy production transactions B_{sell} also includes profits from heating and cooling. Furthermore, the ESS generates additional income by providing more flexibility for the power system in the auxiliary service market. The benefit of ancillary service $B_{subsidy}$ includes frequency-modulation and peak-shaving benefits. For a standalone CAES system, the income from peak shaving is obtained by charging during valley times and discharging during peak times to arbitrage in response to electricity price. As for the integrated CAES system, it is regarded as an auxiliary system equipped with the thermal power plant and adopts the corresponding calculation methods for the CFPP. As there is no uniform fixed calculation method for frequency modulation income, an approximation was used here. In addition, the coal savings and the accompanying pollutant emission reductions owing to more comprehensive energy utilization after integration lead to two additional items in the calculation of the total benefit: the fuel saving profit B_{coal} and the pollutant reduction profit B_{emis}. The total benefit B_{tot} calculation models for the CAES system integrated with the thermal power unit are expressed as below:

$$B_{tot}=B_{sell}+B_{subsidy}+B_{coal}+B_{emis} \tag{8}$$

$$B_{sell}=price_{ele}\int P_{ele}dt+price_{heat}\int Q_{heat}dt+price_{cool}\times\int Q_{cool}dt \tag{9}$$

$$B_{coal}=price_{coal}\int\left(m_{coal,0}-m_{coal}\right)dt \tag{10}$$

$$B_{emis}=\sum\left(price_{emis}\int\left(m_{emis,0}-m_{emis}\right)dt\right) \tag{11}$$

where $price_{ele}$ ($CNY{\cdot}kW^{-1}{\cdot}h^{-1}$), $price_{heat}$ ($CNY{\cdot}GJ^{-1}$), and $price_{cool}$ ($CNY{\cdot}GJ^{-1}$) denote the transaction price of electricity, heating, and cooling energy supply; $price_{coal}$ is the purchase price of the standard coal, $CNY{\cdot}kg^{-1}$; m_{coal} is the coal consumption mass flow rate, $kg{\cdot}s^{-1}$; $price_{emis}$ is the benefit from pollutant emissions reduction, $CNY{\cdot}kg^{-1}$; m_{emis} denote the production of common pollutant emissions along with coal combustion, $kg{\cdot}s^{-1}$.

4.2.3. Economic index

The typical dynamic payback period (DPP) and internal return rate (IRR) were chosen as indicators to evaluate the economics of the system. The investment payback period refers to the minimum

time required to compensate for the original investment with the net cash flow generated by the investment plan. The net cash flow for each year of the investment project is converted into the present value based on the benchmark rate of return in the calculation of DPP. Hence, DPP is more accurate and practical. IRR is the discount rate when the total present value of capital inflows is equal to the total value of the capital flow and the net present value is equal to zero. It can reflect the degree of the profit of the unrecovered investment in each year of the project life [41]. A larger IRR means better benefits for the project investors. These two indexes can be calculated using Eqs. (12) and (13).

$$\sum_{n=0}^{\mathrm{DPP}} \frac{\mathrm{CI}_n - \mathrm{CO}_n}{(1+r)^n} = 0 \tag{12}$$

$$\sum_{n=0}^{N} \frac{\mathrm{CI}_n - \mathrm{CO}_n}{(1+\mathrm{IRR})^n} = 0 \tag{13}$$

where CI_n and CO_n are the cash inflow and outflow in the nth operation year, r is the discount rate, and N is the life cycle of project.

5. Thermodynamic analysis and discussion

The following research aims to assess the system performance and analyze the thermodynamic characteristics under these three typical operation modes. The analysis was carried out based on the following assumption: The main steam parameters of the CFPP were kept the same before and after integration with the CAES system. Different working conditions of the CFPP were studied to draw general conclusions.

5.1. Power generation

In the power generation mode, all the heat generation and heat absorption of the CAES system flows into/from different positions in the steam and water circulation of the CFPP. Hence, possible coupling schemes were discussed considering working conditions of the CFPP.

5.1.1. Scheme discussion of charge process

After integration with the CFPP, the total compression heat produced by the CAES system is cascade used via three-stage intercoolers in accordance with the temperature grade. As shown in Fig. 1, the positions of A_{in} and A_{out} are fixed. The possible schemes for the second- and third-stage coolers are shown in Fig. S3 in Appendix A. Thus, there are six optional schemes for the position combinations of B_{in} and B_{out}, and three possible schemes for the positions of C_{out}. The enthalpy increment of the scheme that injects heated water by air to the inlet of feedwater heater (HTR)-7 is small, requiring a greater mass flow rate of water. For the operation safety of the CFPP, it is abandoned. As the coupling positions of the second- and third-stage coolers are independent, there are 18 potential coupling schemes in total, numbered from s1 to s18. Detailed information on these schemes was provided in Table S4 in Appendix A. It can be seen that the integration scheme is determined by the positions of B_{in}, B_{out}, and C_{out}.

For all schemes, the working conditions of the CAES subsystem remained unchanged, and the parameters of the thermal power unit were varied owing to the different combinations of the two cycles. Hence, the heat rate of the thermal power unit is used to represent the overall system performance in the comparative analysis. Because the CAES charge mode is always activated in valley times and the CFPP normally works at lower conditions, to cater to the actual operation demand, six working conditions, varying from 35% to 60% turbine heat acceptance (THA) working conditions of the original CFPP before integration, were considered and separately calculated. It can be seen that the heat rate is decreased for all schemes and all working conditions because some steam for feedwater preheating is pushed out with the compression heat flowing in. These schemes were classified, compared, and analyzed to explore their effects and regularity.

The total recovered compression heat is divided into three parts and separately used. For all the schemes, the heat exchange in the first-stage cooler is the same, and the position of B_{in} decides the heat allocation in the second- and third-stage coolers. When the position of B_{in} is fixed, the positions of B_{out} and C_{out} reflect the effect of the configuration of the cycle integration on the system performance for the same amount heat exchange with the CAES system. Based on the above analysis, the effects of B_{in}, B_{out}, and C_{out} are separately discussed.

Fig. 2 shows that when the location of B_{in} is the same, for selection of the positions of both B_{out} and C_{out}, increasing the backwater temperature has a positive effect on the system performance. This regularity is applicable for both the second- and third-stage coolers. For example, when the locations of B_{in} and B_{out} are fixed, such as in schemes s1, s2, and s3, the coupling schemes for first- and second-stage coolers are the same, whereas the backwater of the third-stage cooler flows into different temperature-grade locations in the feedwater system. With the increase in the backwater temperature in the third-stage cooler (i.e., $T_{C_{out},s1} > T_{C_{out},s2} > T_{C_{out},s3}$), the heat rate of CFPP is ranked as $HR_{s1} < HR_{s2} < HR_{s3}$. Hence, the reduction in the heat rate compared with that of the original CFPP is ranked as $\Delta HR_{s1} > \Delta HR_{s2} > \Delta HR_{s3}$. Similarly, when the location of B_{in} and C_{out} are unchanged, such as schemes s1, s4, and s7, the coupling schemes for the first- and third-stage coolers are the same, whereas that of the backwater for the second-stage cooler is different. With the increase in the backwater temperature in the second-stage cooler (i.e., $T_{B_{out},s1} < T_{B_{out},s4} < T_{B_{out},s7}$), the performance of the CFPP is ranked as $\Delta HR_{s1} < \Delta HR_{s4} < \Delta HR_{s7}$.

The effects of B_{in} were also studied. The B_{in} position affects the total heat exchange amount of the second- and third-stage coolers. From the calculation results, it can be found that the lower water temperature in B_{in} contributes to a better performance. The reason is that more compression heat is injected into the high section of the feedwater system when the second-stage cooler draws lower-temperature water from the feedwater system as the cold resource. For example, for schemes s7, s13, and s16, the positions of B_{out} and C_{out} are the same, whereas the positions of B_{in} are different. With the increase in the water temperature in B_{in} (i.e. $T_{B_{in},s7} < T_{B_{in},s13} < T_{B_{in},s16}$), the heat rate reduction of the CFPP is ranked as $\Delta HR_{s7} > \Delta HR_{s13} > \Delta HR_{s16}$, respectively.

Based on the above analysis, it is recommended to increase the proportion of the heat distribution that flows into the high-temperature sections in the feedwater system and in the meantime raising the backwater temperature as possible for a better performance. This refined regularity is almost applicable to all working conditions of the CFPP. Based on the above analysis, the optimal coupling scheme is s7 for the charge process with consideration on working conditions of the CFPP. In addition, for all schemes, increased thermo-economic benefits are produced by integration with the CAES system when the CFPP works at a lower condition.

5.1.2. Scheme discussion of discharge process

In the discharge process, three-stage expanders and two-stage heat preheaters are used. Pressurized air is cascade preheated by water and extraction steam. As shown in Fig. S4 in Appendix A, the position of D_{in} can be chosen from the deaerator (DEA) inlet, HTR-5 inlet, HTR-6 inlet, and HTR-7 inlet. For all schemes, the backwater is injected into the condenser; hence, the position of D_{out} remains the same. For the second-stage heater, the position of E_{in} can choose from either the first-stage or second-stage extraction

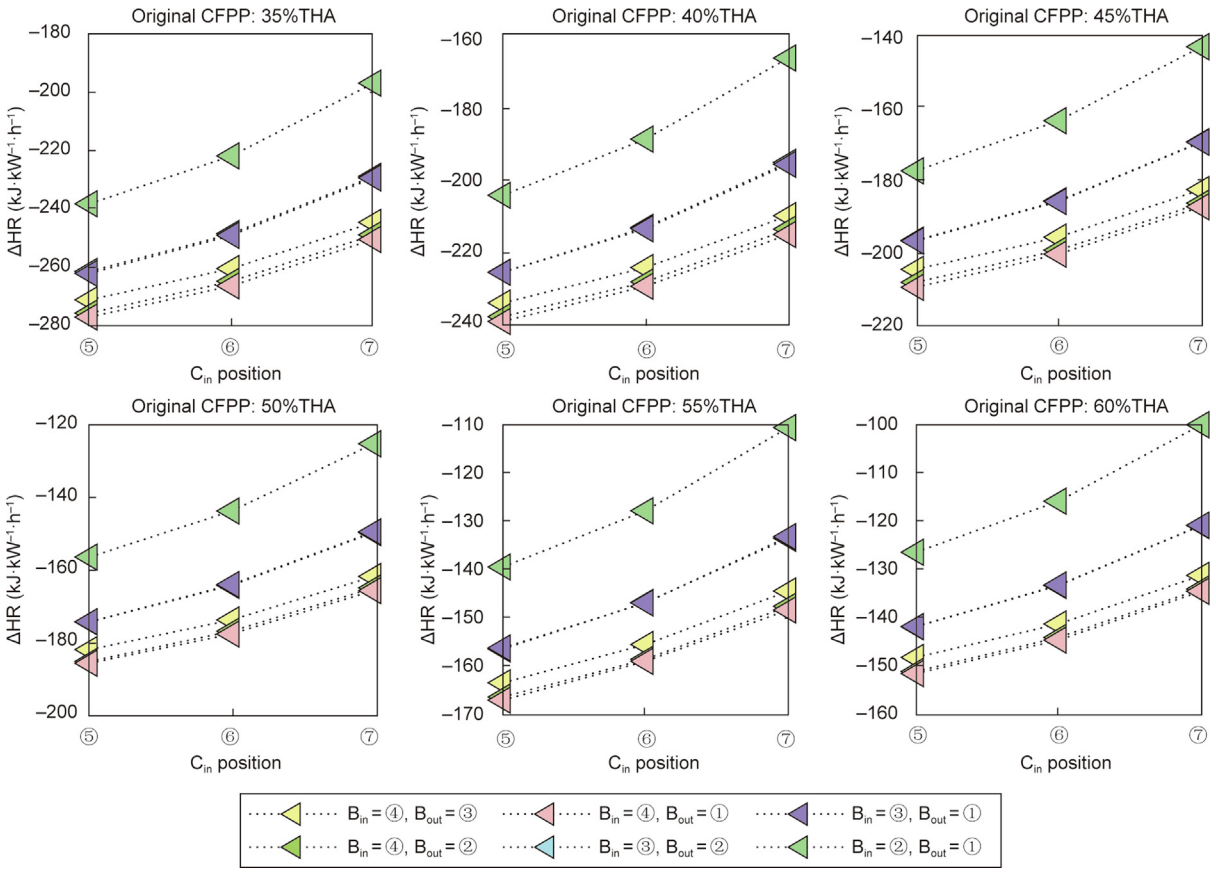

Fig. 2. Effects of positions of B_{in}, B_{out}, and C_{out} on ΔHR.

steam. The steam from other stages does not meet the temperature demand and were not considered in this study. After preheating, the water flows into the corresponding drain cooler. Hence, the position of E_{out} is determined by E_{in}. Totally, there are eight schemes and they are specified by s1–s8 as described in Table S5 in Appendix A. Because the CAES discharge subsystem always works at peak periods, hence, the CFPP normally works at higher conditions, to cater to the actual operation demand, six working conditions of the original CFPP from 75% to 100% THA were considered here to obtain general conclusions.

It can be seen that the system performance is affected by the positions of D_{in} and E_{in}, and they are discussed. Fig. 3 displays the difference of heat rate compared with those of the original CFPP without integration under different working conditions. Because some heat energy is extracted from the circulation for air preheating, the power production is reduced, and accordingly the HR of the unit is higher than that of the original unit. Hence, the values of ΔHR are positive for all schemes. For the first comparison situation that the position of D_{in} is fixed and E_{in} varies, the negative influence can be reduced if the steam extraction point away from the steam turbine inlet is adopted, for example, $\Delta HR_{s1} > \Delta HR_{s2}$. For the second comparison situation that the position of E_{in} is fixed and D_{in} varies, the system performs better performance with a high heat source temperature at position D_{in}, for example, $\Delta HR_{s1} < \Delta HR_{s3} < \Delta HR_{s5} < \Delta HR_{s7}$. This regularity is applicable for different CFPP working conditions. Additionally, for a certain coupling scheme, the ΔHR value lowers if the CFPP works at a higher condition. This is because the temperature grade of the heat source at position D_{in} increases, and more heat can be provided by the feedwater instead of steam. Because more high-energy steam is used to do work and generate power, the integrated system performance is improved.

From the above results and analysis, we concluded that the system performance behaves better if the air is preheated to as high temperature as possible using the low-grade water from the feedwater system, and steam is used as a supplement to further heat the air until it reaches the expected temperature. Moreover, for the same amount of heat provided by different stages of steam extraction, using a point away from the steam turbine inlet results in better performance. As such, considering the working conditions of the CFPP, the optimal coupling scheme for the proposed system is s2. In addition, the results of analysis indicate that the performance of the proposed system performance can be enhanced under a high working condition of the CFPP.

5.1.3. Analysis of optimal integration

Taking an example of a typical scenario, the thermodynamics of the integrated system for a complete storage cycle were analyzed based on the optimal scheme. The scenario is set as that the original CFPP under 35% THA working condition was integrating with the CAES charge subsystem, and the original CFPP under 100% THA working condition was integrating with the discharge subsystem. The detailed calculation results were displayed in Tables S6 and S7 in Appendix A. The relative values of the main parameters of the integrated CFPP in comparison with those of the original CFPP were displayed in Fig. S5 in Appendix A. It can be seen that the electric energy generated by the CFPP increases by 10.74 MW·h due to the compression heat injected during the charging process. Additionally, the integration results in a reduction of 2.85 tonnes coal consumption for one cycle. The total on-grid power generation

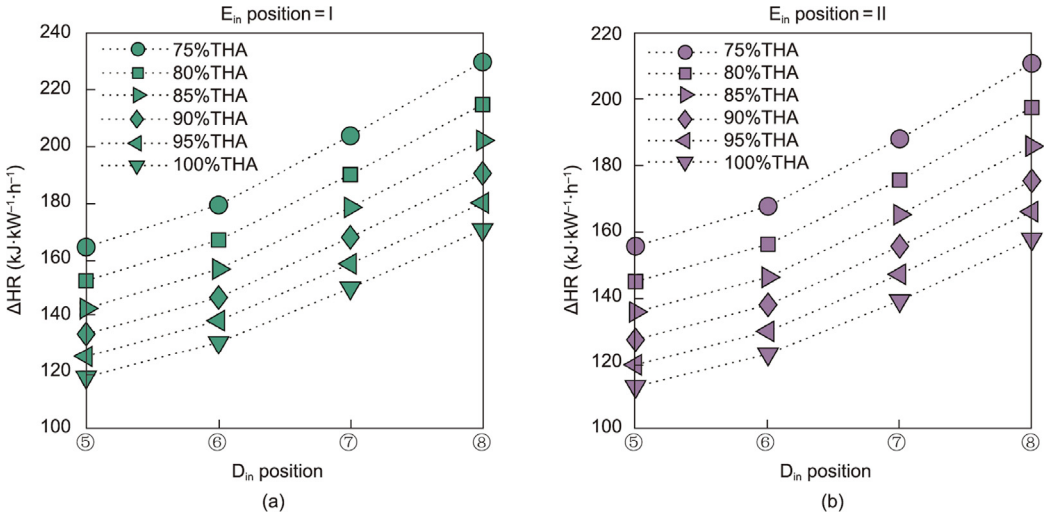

Fig. 3. Effect of D_{in} and E_{in} positions on ΔHR. (a) D_{in} position affect when E_{in} position = I; (b) D_{in} position affect when E_{in} position = II.

of the thermal power plant is reduced by 60.66 MW·h in total. As for the discharge phase, the electric energy output of CFPP deceases 12.55 MW·h as a result of pressurized air heating. Nevertheless, the total on-grid electric energy is still increased by 33.55 MW·h. After integration with the CFPP, the SPE is reduced to 55.32%. This is because the high-temperature portion of compression heat is used to preheat the feedwater before entering into the boiler. As a result, the increase in the electric production of the thermal power unit in the charge stage is less than its reduction in the discharge stage, which then influences the total power generation in a cycle. However, when the fuel-saving benefit is considered in the calculation, the system RTE can be increased from 64.58% to 66.82%, with an apparent increment of 2.24%. The results indicate that the integration of CFPP and CAES system has benefit in enhancing energy utilization.

5.2. Cogeneration of heat and power

In the heat–power operation mode, the compression heat is cascaded utilized to flow into the steam–water circulation and supply heat. The investigation into the effect of heat utilization on the system effect was divided into two parts: the effect on the performance of the heat allocation between the first- and second-stage coolers, and between the second- and third-stage coolers. The heat allocation and use for the same amount of thermal energy were changed by changing the terminal temperature difference (TTD) of the first-stage heat exchanger $TTD_{IC,1}$ and the second-stage heat exchanger $TTD_{IC,2}$ through the corresponding regulating valves.

5.2.1. Effect of $TTD_{IC,1}$ analysis

To study the effect of the heat allocation between the total heat exchange in the first-stage cooler $Q_{c,1}$ and second-stage cooler $Q_{c,2}$, we fixed the temperature difference between the second- and third-stage cooler $Q_{c,3}$ and increased that of the first-stage cooler. Fig. S6 in Appendix A shows the proportions of $Q_{c,1}$, $Q_{c,2}$, and $Q_{c,3}$ in the total recovered compression heat variation with $TTD_{IC,1}$ varying under the different working conditions of the CFPP. We found that the amount of $Q_{c,1}$ which is used to preheat the feedwater before flowing into the boiler decreases; $Q_{c,2}$, which flows into the steam and water circulation increases; and the heating supply $Q_{c,3}$ to satisfy the user heat demand is fixed when increasing $TTD_{IC,1}$ for all conditions. Because a higher working condition of the CFPP means a higher feedwater temperature, the difficulty of heat exchange increases in the first two stage coolers. Hence, the proportion of both $Q_{c,1}$ and $Q_{c,2}$ lower, while that of $Q_{c,3}$ increase for increasing working conditions of the CFPP.

The effect of $TTD_{IC,1}$ on the power generation difference $\Delta P_{CFPP,ch}$ of the thermal power unit before and after integration is shown in Fig. S7 in Appendix A, and the variation of total coal savings is shown in Fig. S8 in Appendix A. For a certain condition, more heat flows into the feedwater system, contributing a higher power output as less steam needs to be extracted from the turbine stage. However, the actual temperature of the feedwater flowing into the boiler decreases. As a result, the coal consumption increases to ensure the main steam parameters remain unchanged, and the coal saving benefit is reduced.

Regarding the total effect on system performance, the SPE tends to increase with increasing $TTD_{IC,1}$ (Fig. 4); then, the energy storage cost reduces. However, from the comprehensive energy use as indicated by RTE, the performance of thermodynamic economy performs better using the compression heat as a complementary heat source to reduce coal consumption in comparison with directly flowing into the feedwater system. This conclusion is applicable for CAES charge subsystem integration with all the studied working conditions of the CFPP. Additionally, it can be seen that the values of SPE and RTE under high working conditions of CFPP are notably larger.

5.2.2. Effect of $TTD_{IC,2}$ analysis

The effect of the heat allocation between $Q_{c,2}$ and $Q_{c,3}$ was studied. The temperature differences in both the first- and third-stage heat exchangers were kept constant, while the temperature difference in the second-stage $TTD_{IC,2}$ was changed by adjusting the mass flow rate of the cold water. With an increasing in $TTD_{IC,2}$, the heat injected into the steam and water circulation $Q_{c,2}$ through the second-stage heat exchanger is reduced, and the heating supply $Q_{c,3}$ increases as shown in Fig. S9 in Appendix A. As less compression heat is absorbed by the CFPP cycle if $TTD_{IC,2}$ increases, the power generation ability tends to decline as Fig. S10 in Appendix A shown. Hence, the SPE values accordingly reduce. However, the positive benefits from heating outweigh its adverse effects on power production. Consequently, the RTE values tend to increase, as shown in Fig. 5.

The thermal calculation results under other CFPP working conditions exhibited the same phenomenon, so the above conclusions are further validated. In addition, when the CFPP works under a

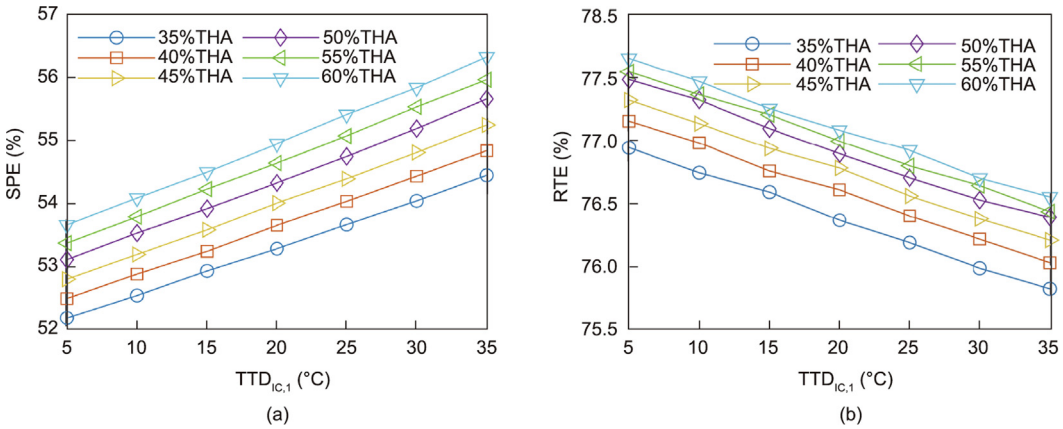

Fig. 4. Variation in (a) SPE and (b) RTE with $TTD_{IC,1}$.

higher condition, the effect of $TTD_{IC,2}$ is weakened because the temperature of the feedwater in the corresponding coupling positions increase with the increasing working conditions. A higher cold source temperature grade reduces the maximum possible heat exchange in the first two stages of the heat exchangers. Hence, the influence of $TTD_{IC,2}$ on performance becomes weaker. However, the cogeneration of heat and power contributes to a considerable increase in efficiency under all working conditions. From the above results and analysis, the reasonable priority in the compression heat use is concluded that it should be absorbed by the feedwater before flowing into the boiler to increase its temperature, and the rest heat is preferred to supply heat to enhance the system efficiency. The allocation proportions of heat between heating and flowing into the CFPP cycle can also be adjusted to satisfy the actual heat demand.

5.3. Cogeneration of cooling and power

Because the integration with a CFPP breaks the thermal coupling between the energy storage and release processes, the inlet temperature of the air expanders can be adjusted according to the actual demand. The working characteristics of expanders decide that the outlet air temperature correspondingly reduces if the inlet temperature is lowered; hence, the cold air has the potential to provide cooling energy for users. The effect of the inlet air temperature on the system during the discharge process was studied to explore and analyze the cooling–power cogeneration characteristics. To eliminate the influence of the charging process, the operation mode of the CAES and the working conditions of the CFPP during the charging process were kept the same as described in Section 5.1.3.

The inlet air temperature of expander $T_{e,in}$ was set to vary from 140 to 180 °C. With the decrease in $T_{e,in}$, the outlet air temperature for both the high- and low-pressure expanders decrease. Because the working state deviates from the design point, the working efficiency of air expanders and the power generation of the CAES system accordingly reduces. However, the lower $T_{e,in}$ provides benefits in producing more cooling energy. Additionally, less heat is absorbed by the pressurized air, and the power generation ability of CFPP is strengthened. As an example, $T_{e,in}$ = 140 °C and the original CFPP works under the 80% THA condition, 3.26 MW of cooling power is produced at the expense of 3.64 MW power generation reduction by the expanders and 0.50 MW power generation reduction of the proposed system. It can be seen that the cost for cooling energy generation is relatively low under the dual influence of $P_{CFPP,dis}$ and P_e. Fig. S11 in Appendix A displayed the cooling power generated by the CAES system and the total system power generation variation $\Delta P_{tot,dis}$ compared with that of the original CFPP in the discharge process under different working conditions.

From the system performance perspective, because cooling is generated at the expense of partial electricity output, the SPE reduces (Fig. 6). However, the RTE increases because of cooling supply. Furthermore, the RTE increases with increasing cooling generation. In the aforementioned case, RTE increases by 2.13%, indicating that although a small amount of power output is sacrificed, the cogeneration of electricity and cooling power still

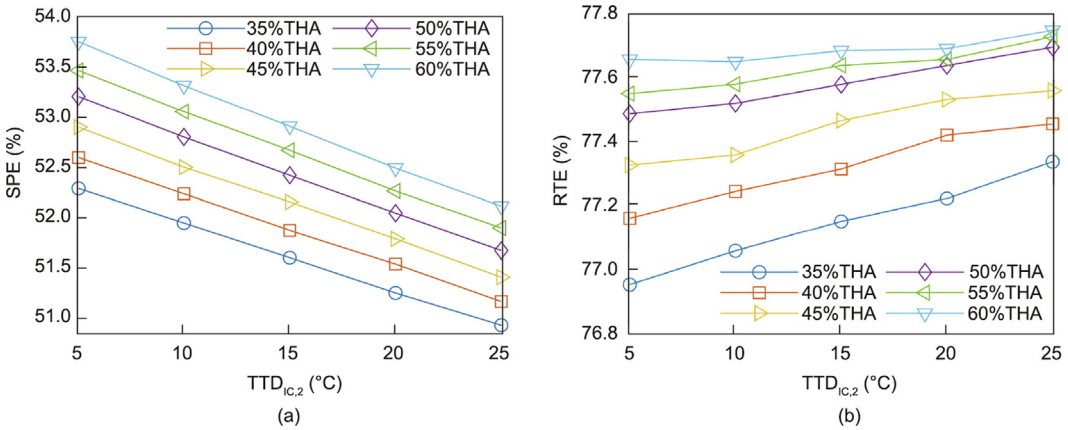

Fig. 5. Variation in (a) SPE and (b) RTE with $TTD_{IC,2}$.

positively affects the system performance. The results under the other working conditions exhibited the same tendency. This means that the above conclusion is applicable for different operating conditions and further proves the advantages of the system; the performance enhancement is greater when the CFPP operates at higher load ratio.

6. Techno-economic analysis

As a new system, a comprehensive consideration of its future marketing is required. In this study, the techno-economics of the proposed trigenerative system based on the CFPP–CAES combined cycle were analyzed. A typical middle region was adopted as an application scenario with cooling energy demand in summer, heating demand in winter, and only electricity needs in transition seasons. The system was assumed to operate for 300 days per year. The last periods for the three typical operation modes were equal, and the CAES system worked for one cycle per day. The expander inlet temperature was set as 150 °C. To consider the effects of the CFPP working conditions, we assumed that the CFPP worked under a combination of two typical conditions with different peak–valley characteristics in each season. For Condition 1, the original conditions of the CFPP before integration with the CAES charge and discharge subsystems were separately set as 40% and 100% THA, respectively; for Condition 2, the original CFPP conditions before integration with the CAES charge and discharge subsystems were set as 50% and 80% THA, respectively. Each season in Conditions 1 and 2 was assumed to have the same lasting days.

The annual energy generation is presented in Table 3 and the results of the system cost and benefit of each item are listed in Table 4. It can be seen that 2.19 million CNY is saved owing to the removal of the thermal storage tanks. After coupling and integration with the thermal power plant, the fixed initial cost of the CAES system can be reduced by 3.02 million CNY. For the standalone CAES system, the purchase price of electricity during valley periods was 0.3 CNY·kW^{-1}·h^{-1}, and the selling price during peak periods was 0.8 CNY·kW^{-1}·h^{-1}. For the proposed system, the feed-in tariff for the CFPP was set to 0.36 CNY·kW^{-1}·h^{-1}; the heating and cooling supply prices were 90 and 115 CNY·GJ^{-1}, respectively; the coal purchase price was 1000 CNY·t^{-1}. The subsidy policy in the calculation refers to the typical power auxiliary service market operation rules in northeast China [42]. The results showed that the energy storage cost increased by 0.146 million CNY. Moreover, owing to the multiple profits from integration, the total annual benefit of the CAES system increased from 14.972 to 17.134 million CNY, an increase of nearly 14.43%. The synergistic benefits of cost savings and increased benefits promote better performance in system economics. Regarding the economic indicators, the DPP reduces from 21.70 to 10.37 years, a reduction of 11.33 years. In addition, the internal rate of return increases from 9.06% to 14.26%, which is an increase of 5.20% compared with the standalone CAES plant. These results demonstrated that the proposed integration of the CAES system and CFPP provides dominant advantages in both thermal economy and investment economy.

To explore the system investment value in regions with different seasonal characteristics, the effects of lasting periods of different operation modes were investigated and analyzed. The duration of power generation, cogeneration of heat and power, and cogeneration of cooling and power modes are denoted as d_{ele}, d_{heat}, and d_{cool}, respectively. In this study, the total operation days for the integrated system in a year were fixed; hence, $d_{ele} + d_{heat} + d_{cool} = d_{total}$.

Fig. 7 shows the variation in DPP and IRR with regional seasonal characteristics. The values of DPP decrease with increasing d_{cool} when the heat–power mode operation period is fixed, and the values of IRR are the opposite. For the case where $d_{heat} = 75$, the DPP varies from 15.93 to 13.37 years and IRR varies from 10.74% to 11.99% when d_{ele} varies from 225 to 0 days. Similarly, when the operation days of cooling–power mode is fixed, the economic performance of the system improves with increasing d_{heat}. The above results indicated that multiple-energy production contributes the system economy compared with that of power generation only. Additionally, for a certain d_{ele}, a higher d_{heat} is more economical. This means that the system can obtain more profits from heat and power cogeneration because cold energy is produced at the cost of some electricity output reduction, so the whole benefit is influenced. From the above analysis, we found that for most application scenarios, the economic performance of the integrated system is better than that of the standalone CAES system. Furthermore, the proposed integrated CAES and CFPP trigenerative system is more investable in areas with a cold climate.

7. Conclusions

Considering their characteristics and shortages, this paper firstly proposed the concept of the CFPP–CAES combined cycle and analyzed its thermodynamic mechanism to provide deep insights into this novel integration. Based on that, a trigenerative system was put forward and thermodynamic analysis for three typical operation modes under different working conditions were performed to evaluate the novel system and reveal its heat conversion and use characteristics. Finally, economic evaluation

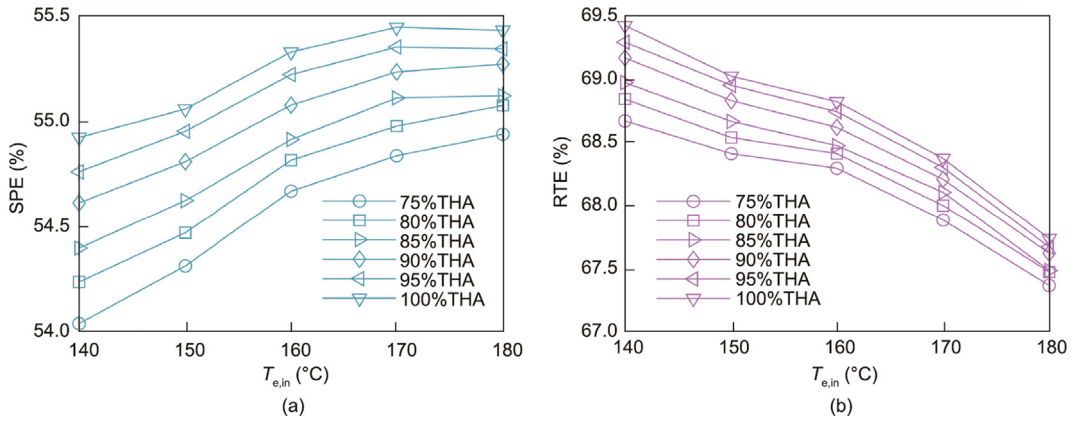

Fig. 6. Variation in (a) SPE and (b) RTE with $T_{e,in}$.

Table 3
Energy generation results after integration with CFPP.

Season	Electricity consumption (MW·h)	Electricity production (MW·h)	Heat production (GJ)	Cooling production (GJ)	Coal saving (t)
Summer	5950.00	3316.93	0	2275.03	224.73
Transitions	5950.00	3344.82	0	0	245.46
Winter	6349.84	3344.82	10818.05	0	245.46

Table 4
Cost and benefit results.

Cost and benefit	Item	Value ($\times 10^6$ CNY)	
		Independent mode	Integrated mode
Initial cost	C_{eq}	40.35	38.16
	C_{land}	2.50	2.00
	C_{con}	6.05	5.72
Operation cost	C_{ele}	6.42	6.57
	C_{labor}	1.20	0.96
	C_{ma}	0.98	1.47
Benefit	B_{sell}	11.06	4.84
	B_{coal}	0	0.72
	B_{emis}	0	0.01
	$B_{subsidy}$	3.91	11.58

considering application scenario effect was analyzed to provide guidance for investment and marketing. The main conclusions are summarized as follows:

(1) The effects regularity of the different schemes on the system performance were identified, and the optimal scheme was determined considering the working conditions. When integrating the CAES charge subsystem with the CFPP, extracting water from the low-temperature points in the feedwater system as a cold source while increasing the backwater temperature is beneficial for better performance; for the discharge phase, the priority should be preheating the pressurized air with the low-grade water in the feedwater system and the steam as a supplement. A detailed thermal analysis of an example scenario shows that 2.85 tonnes of coal can be saved for per cycle, and the RTE increases by 2.24% compared with that of the standalone CAES system.

(2) Combined heat and power generation can further enhance the system efficiency RTE to more than 77.5%, and the benefit is increased when the CFPP works at high load ratio conditions. In addition, the degree of contribution of the compression heat use in the three-stage heat exchangers to the performance improvement was obtained: preheating the feedwater before the boiler should be prioritized for supplying heat prior to flowing into the feedwater system.

(3) The cogeneration of cooling and power also contributes to an improvement in the system performance. The amount of cooling energy generated, the power generation variation of both the CAES system and the CFPP, and the reduction in the total power generated by the system due to the cooling supply under different working conditions were quantitatively studied. Because cooling energy production is produced at the expense of electric energy generation, its degree of contribution to system performance is lower than that of the heat and power cogeneration mode. In general, the RTE can reach to 69%, and the benefit increases if the CFPP operates at a higher load ratio.

(4) Integration with the CFPP improves the economics benefits compared with the standalone CAES system. The DPP can be shortened by 11.33 years and the IRR increases by 5.20% under a typical application scenario. In addition, the effect of application scenarios was discussed to explore the applicability of the advanced system in different regions from a techno-economics perspective. The results indicated that the proposed system can obtain increased profits in multi-energy scenarios, particularly for the heat and power cogeneration.

In this paper, we qualitatively analyzed and quantitatively demonstrated the technical advantages of integrating CFPP and CAES systems from both thermo-economic and techno-economic

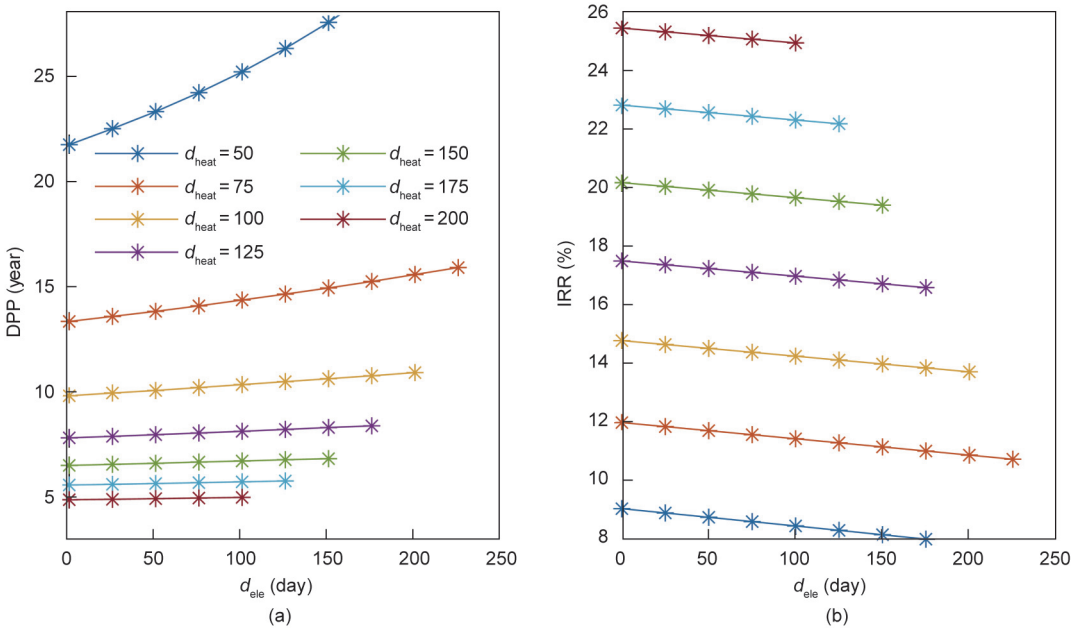

Fig. 7. Effect of d_{ele} and d_{heat} on (a) DPP and (b) IRR.

perspectives. The results and conclusions provide guidance for novel system design, operation and investment.

Compliance with ethics guidelines

Jiajia Li, Peigang Yan, Guowen Zhou, Xingshuo Li, Qiang Li, Jinfu Liu, and Daren Yu declare that they have no conflict of interest or financial conflicts to disclose.

Appendix A. Supplementary data

Supplementary data to this article can be found online at https://doi.org/10.1016/j.eng.2023.08.011.

References

[1] Mitchell C. Momentum is increasing towards a flexible electricity system based on renewables. Nat Energy 2016;1(2):15030.
[2] International Energy Agency (IEA). World energy outlook 2020. Report. Paris: International Energy Agency; 2020.
[3] National Energy Administration. 2022 energy work guidance [Internet]. Beijing: National Energy Administration; 2022 Mar 17 [cited 2023 Aug 1]. Available from: https://www.gov.cn/zhengce/zhengceku/2022-03/29/content_5682278.htm. Chinese.
[4] National Development and Reform Commission; National Energy Administration. Opinions on improving the system, mechanism and policy measures for green and low carbon energy transformation [Internet]. Beijing: National Development and Reform Commission; 2022 Jan 30 [cited 2023 Aug 1]. Available from: https://www.ndrc.gov.cn/xxgk/zcfb/tz/202202/t20220210_1314511_ext.html. Chinese.
[5] Li Z, Qiao X, Miao Z. Low load performance of tangentially-fired boiler with annularly combined multiple airflows. Energy 2021;224:120131.
[6] Eser P, Singh A, Chokani N, Abhari RS. Effect of increased renewables generation on operation of thermal power plants. Appl Energy 2016;164:723–32.
[7] Garoarsdottir S. Improving the flexibility of coal-fired power generators: impact on the composition of a cost-optimal electricity system. Appl Energy 2018;209:277–89.
[8] Zaloudek FR, Reilly RW. An assessment of second-generation compressed-air energy-storage concepts. Report. Washington, DC: US Department of Energy; 1982. Report No.: DE82019513.
[9] Fort JA. Thermodynamic analysis of five compressed-air energy-storage cycles Report. Washington, DC: US Department of Energy; 1983.
[10] Soltani M, Kashkooli FM, Jafarizadeh H, Hatefi H, Gharali K, Nathwanli J, et al. Diabatic compressed air energy storage (CAES) systems: state of the art. In: Encyclopedia of energy storage. Amsterdam: Elsevier; 2022. p. 173–87.
[11] Tong Z, Cheng Z, Tong S. A review on the development of compressed air energy storage in China: technical and economic challenges to commercialization. Renew Sustain Energy Rev 2021;135:110178.
[12] Jia G, Xu W, Cai M, Shi Y. Micron-sized water spray-cooled quasi-isothermal compression for compressed air energy storage. Exp Therm Fluid Sci 2018;96:470–81.
[13] Jafarizadeh H, Soltani M, Nathwani J. Assessment of the Huntorf compressed air energy storage plant performance under enhanced modifications. Energy Convers Manage 2020;209:112662.
[14] Razmi AR, Janbaz M. Exergoeconomic assessment with reliability consideration of a green cogeneration system based on compressed air energy storage (CAES). Energy Convers Manag 2020;204:112320.
[15] Razmi A, Soltani M, Aghanajafi C, Torabi M. Thermodynamic and economic investigation of a novel integration of the absorption–recompression refrigeration system with compressed air energy storage (CAES). Energy Convers Manage 2019;187:262–73.
[16] Yao E, Wang H, Wang L, Xi G, Maréchal F. Multi-objective optimization and exergoeconomic analysis of a combined cooling, heating and power based compressed air energy storage system. Energy Convers Manage 2017;138:199–209.
[17] Alirahmi SM, Mousavi SB, Razmi AR, Ahmadi P. A comprehensive techno–economic analysis and multi-criteria optimization of a compressed air energy storage (CAES) hybridized with solar and desalination units. Energy Convers Manage 2021;236:114053.
[18] Pan P, Zhang M, Peng W, Chen H, Xu G, Liu T. Thermodynamic evaluation and sensitivity analysis of a novel compressed air energy storage system incorporated with a coal-fired power plant. Entropy 2020;22(11):1316.
[19] Zhang L, Cui J, Zhang Y, Yang T, Li J, Gao W. Performance analysis of a compressed air energy storage system integrated into a coal-fired power plant. Energy Convers Manage 2020;225:113446.
[20] Li B, Chen J, Li CX, Chen HS, Ji L. Research on coupling schemes of a compressed air energy storage system and thermal power unit. J Chin Soc Power Eng 2021;41(03):244–50. Chinese.
[21] Wang Y, Lv K, Ma TS, Ju WP, Zhang JY, Xu PJ, et al. Analysis of compressed air energy storage system coupled with coal-fired power unit. Therm Power Gener 2021;50(08):54–63. Chinese.
[22] Wang X, Guo H, Zhang H, Xu Y, Liu YJ, Chen HS. Analysis of energy coupling characteristics between cogeneration units and compressed air energy storage integrated systems in thermal power plants. Energy Stor Sci Technol 2021;10(02):598–610. Chinese.
[23] Fiebrandt M, Röder J, Wagner HJ. Minimum loads of coal-fired power plants and the potential suitability for energy storage using the example of Germany. Int J Energy Res 2022;46(4):4975–93.
[24] Zhou Y, Zhai Q, Wu L. Multistage transmission-constrained unit commitment with renewable energy and energy storage: implicit and explicit decision methods. IEEE Trans Sustain Energy 2020;12(2):1032–43.
[25] Kreid DK. Technical and economic feasibility analysis of the no-fuel compressed air energy storage concept. Report. Richland: Battelle Pacific Northwest Labs; 1976.
[26] Budt M, Wolf D, Span R, Yan J. A review on compressed air energy storage: basic principles, past milestones and recent developments. Appl Energy 2016;170:250–68.
[27] Li P, Hu Q, Han Z, Wang C, Wang R, Han X, et al. Thermodynamic analysis and multi-objective optimization of a trigenerative system based on compressed air energy storage under different working media and heating storage media. Energy 2022;239(Pt D):122252.
[28] Sanjay Y, Singh O, Prasad BN. Energy and exergy analysis of steam cooled reheat gas–steam combined cycle. Appl Therm Eng 2007;27(17–18):2779–90.
[29] Minutillo M, Lavadera AL, Jannelli E. Assessment of design and operating parameters for a small compressed air energy storage system integrated with a stand-alone renewable power plant. J Energy Storage 2015;4:135–44.
[30] Cheayb M, Gallego MM, Tazerout M, Poncet S. Modelling and experimental validation of a small-scale trigenerative compressed air energy storage system. Appl Energy 2019;239:1371–84.
[31] Li R, Wang H, Zhang H. Dynamic simulation of a cooling, heating and power system based on adiabatic compressed air energy storage. Renew Energy 2019;138:326–39.
[32] Lu S, Lin R. Gas turbine steady-state design and off-design characteristic general model. J Eng Thermophys 1996;17:407–9.
[33] Kumar R. Thermodynamic modeling and validation of a 210-MW capacity coal-fired power plant. Iran J Sci Technol Trans Mech Eng 2016;40(3):233–42.
[34] Mohammadi A, Ahmadi MH, Bidi M, Joda F, Valero A, Uson S. Exergy analysis of a combined cooling, heating and power system integrated with wind turbine and compressed air energy storage system. Energy Convers Manage 2017;131:69–78.
[35] Jiang R, Yin H, Peng K, Xu Y. Multi-objective optimization, design and performance analysis of an advanced trigenerative micro compressed air energy storage system. Energy Convers Manage 2019;186:323–33.
[36] Jannelli E, Minutillo M, Lavadera AL, Falcucci G. A small-scale CAES (compressed air energy storage) system for stand-alone renewable energy power plant for a radio base station: a sizing-design methodology. Energy 2014;78:313–22.
[37] Rashid K, Safdarnejad SM, Ellingwood K, Powell KM. Techno-economic evaluation of different hybridization schemes for a solar thermal/gas power plant. Energy 2019;181:91–106.
[38] Couper JR, Penney WR, Fair JR. Chemical process equipment-selection and design. 2nd ed. Houston: Gulf Professional Publishing; 2009.
[39] Ulrich GD. A guide to chemical engineering process design and economics. New York City: Wiley; 1984.
[40] Zhang X, Zeng R, Deng Q, Gu X, Liu H, He Y, et al. Energy, exergy and economic analysis of biomass and geothermal energy based CCHP system integrated with compressed air energy storage (CAES). Energy Convers Manage 2019;199:111953.
[41] You DM. Technical economy and project economic evaluation. Beijing: Tsinghua University Press; 2009. Chinese.
[42] Notice on soliciting opinions on the operation rules of northeast electric power auxiliary service market. Report. Shenyang: Northeast China Energy Regulatory Bureau of the National Energy Administration of the People's Republic of China; 2020. Chinese.